Available online at www.sciencedirect.com
SCIENCE DIRECT®
Journal of Solid State Chemistry 178 (2005) 1422–1428
JOURNAL OF SOLID STATE CHEMISTRY
www.elsevier.com/locate/jssc

The origin of the stereochemically active Pb(II) lone pair: DFT calculations on PbO and PbS

Aron Walsh, Graeme W. Watson*

Department of Chemistry, School of Natural Sciences, The University of Dublin Faculty of Science, Trinity College Dublin, Main Building, Dublin 2, Ireland

Received 8 December 2004; received in revised form 14 January 2005; accepted 30 January 2005
Available online 16 March 2005

Abstract

The concept of a chemically inert but stereochemically active $6s^2$ lone pair is commonly associated with Pb(II). We have performed density functional theory calculations on PbO and PbS in both the rocksalt and litharge structures which show anion dependence of the stereochemically active lone pair. PbO is more stable in litharge while PbS is not, and adopts the symmetric rocksalt structure showing no lone pair activity. Analysis of the electron density, density of states and crystal orbital overlap populations shows that the asymmetric electron density formed by Pb(II) is a direct result of anion–cation interactions. The formation has a strong dependence on the electronic states of the anion and while oxygen has the states required for interaction with Pb 6*s*, sulphur does not. This explains for the first time why PbO forms distorted structures and possesses an asymmetric density and PbS forms symmetric structures with no lone pair activity. This analysis shows that distorted Pb(II) structures are not the result of chemically inert, sterically active lone pairs, but instead result from asymmetric electron densities that rely on direct electronic interaction with the coordinated anions.

Keywords: Density functional theory; Electronic structure; Lead oxide; Lone pairs

1. Introduction

Asymmetric electron densities are observed in a wide range of technologically important materials, which contain ions with a valence two less than their group. This includes elements from the bottom of Group 13 (Tl(I)), Group 14 (Pb(II), Sn(II)) and Group 15 (Bi(III)), with the asymmetric electron densities often referred to as a lone pair [1]. A detailed understanding of the electronic structure of such materials would contribute significantly to understanding the properties of these ions and the materials in which they are found.

Pb(II) has long been associated with lone pairs in solid state materials [1]. The Pb(II) $6s^2$ electrons are considered to form a lone pair, filling an orbital created through the hybridization of the 6*s* and 6*p* atomic orbitals. This chemically inert pair of electrons are considered to be sterically active, resulting in distorted crystal structures. PbO exists in both a low temperature phase α-PbO [2] (litharge) and a high temperature phase β-PbO [3] (massicot) formed above 762 K. Litharge is a highly asymmetric crystal structure, which can be seen as a distortion of the eight coordinate CsCl structure. In α-PbO each Pb has four oxygen nearest neighbours, all of which are on the same side of the Pb with a lone pair projected in the opposite direction, Fig. 1a. This sterically active lone pair has always been directly associated with the Pb(II) species, however, other Pb compounds do not display the same distortion in their crystal structures. PbS adopts the rocksalt structure as its thermodynamically stable phase in which the Pb sites are six coordinate and perfectly symmetric [4], Fig. 1b. If the asymmetric electron density produced by PbO was a

*Corresponding author. Fax: +353 1 671 2826.
E-mail address: watsong@tcd.ie (G.W. Watson).

0022-4596/$ - see front matter © 2005 Elsevier Inc. All rights reserved.
doi:10.1016/j.jssc.2005.01.030

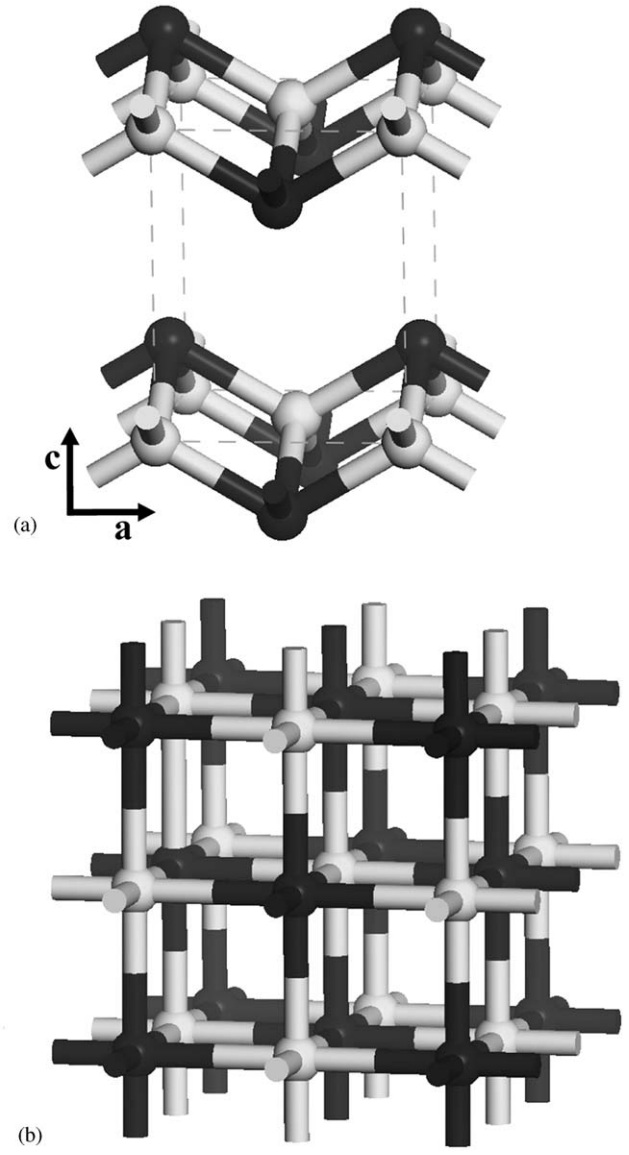

Fig. 1. Illustration of the crystal structure of (a) litharge and (b) rocksalt PbO, Pb atoms are coloured dark and anions are light.

lone pair formed purely by the Pb(II) ion, such a feature would be expected to form in all Pb(II) compounds although this is not the case.

Similar behaviour is also observed for Pb(II) complexes. Two types of Pb(II) coordination are found where coordinated ligands can be identified as being symmetrically distributed around Pb(II) [5] or distorted to one side [6–8] leaving a noticeable void. In this way the Pb(II) lone pair can be stereochemically active or inactive depending on the coordinated ligands [9]. Experimentally the activity of the lone pair is controlled by the bulkiness of the ligands with little consideration of the electronic structure. Simoni-Livny et al. [10] examined the stereochemistry resulting for different ligands in a number of Pb(II) complexes using MP2 with the LANL2DZ basis set. While the stereochemical activity of the lone pair was observed to have a clear anion dependence on transition from $Pb[OH_2]_4$ to $Pb[TeH_2]_4$, no plausible explanation was put forward. Bernasconi et al. [11] examined the polarizibility of a SnO molecule in the gas phase at the GGA level. Wannier decomposition was used to partition the charge density onto individual ions. While hybridization of O(2*p*) with unfilled Sn(5*p*) states is predicted any analysis of the lone pair states is restricted through the limited approach taken, examining only the partitioned charge density.

A detailed study of both α and β-PbO was carried out by Trinquier and Hoffmann [12] using the Extended Hückel Theory. Despite the limitations of the approach, this study yielded insight into both the electronic structure of PbO, examining the band structure and bonding of PbO units starting from dimmers and building up to the three-dimensional solids. They find the intralayer bonding in α-PbO to be stronger than in β-PbO. DFT calculations within a plane wave basis set have been performed on the band structure of α and β-PbO [13]. Only the observed crystal structures were examined, which were held fixed at the experimentally determined structures, and so they were unable to compare the distorted structures of PbO with related undistorted structures which would have allowed direct investigation of the origin of the lone pair.

In previous work [14,15] we have shown that PbO is not a purely ionic material. There are significant interactions between the Pb 6*s* states and the O 2*p* states resulting in filled antibonding orbitals near the Fermi level which have some Pb 6*s* character. A similar picture has been established from density functional theory (DFT) for SnO [16,17], which also adopts the litharge structure and displays an asymmetric electron density. In the case of SnO the observation of the Sn 5*s* states close to the Fermi level is in agreement with recent photoemission data [18] supporting the calculated electronic structure. These studies of PbO and SnO indicate that it is these states close to the Fermi level, and not the main *s* states at lower energy, which give rise to lone pair formation. Raulot et al. have performed DFT calculations on litharge PbO and SnO [19] although their focus was on electron densities and Electron Localisation Functions (ELFs) of lone pairs rather than on their electronic origin. Waghmare et al. [20] used DFT to study the rocksalt chalcogenides of Ge, Pb and Sn and although they observed differences in electronic structure for different anions they could comment on lone pair formation as rocksalt is symmetric.

All of the previous studies were unable to examine the reasoning behind the differences in the observed crystal structures on changing the anion. It is only by examining the differences in the electronic structures of

anions in various crystal phases that both include lone pairs and do not include lone pairs that the reasoning behind the anion dependence of lone pair activity can be established. In this study we investigate for the first time the electronic structure of both PbO and PbS in the rocksalt and litharge structures with a view to fully explaining the lone pair activity of Pb(II) in PbO and the highly symmetric Pb(II) in PbS.

2. Computational methods

The calculations were performed using periodic DFT as implemented in the code VASP [21,22]. The exchange and correlation energy was evaluated within the generalized gradient approximation (GGA) using the parameterization of Perdew et al. [23] (PBE). The valence electrons are expanded in terms of a plane wave basis set with the core electrons (Pb [Xe], O: [He], S: [Ne]) treated using the Projected Augmented Wave approach [24] (based on scalar relativistic all electron calculations). The calculations were checked for convergence with respect to both plane wave cut off (400 and 300 eV were used for PbO and PbS, respectively) and k-point sampling ($4\times4\times4$ and $6\times6\times6$ grids were used for rocksalt and litharge, respectively). Optimization at a series of volumes was performed, allowing the atomic positions, the lattice vectors, and angles to relax within constrained total volume. The resulting energy volume curve was fitted to the Murnaghan equation of state to obtain the equilibrium cell volume. This approach was taken to avoid the problem of the Pulay stress and changes in basis set that occur in plane wave calculations on volume changes [25].

3. Results and discussion

Table 1 shows the equilibrium lattice vectors, binding energies (energy relative to atoms), and nearest Pb-anion distances. Both PbO and PbS have local minima in the rocksalt structure; however, while PbO is more stable in the litharge structure, PbS is not. Optimization of PbS starting with the litharge structure of PbO scaled for the anion, resulted in an expansion of the a and b vectors and contraction of the c vector (see "litharge PbS" in Table 1). This is an attempt to create a symmetric Pb site by relaxing toward the undistorted CsCl structure. The litharge structure can be thought of as the CsCl structure with a $\sqrt{2}\times\sqrt{2}$ expansion and the c vector elongated to create a layered structure. Relaxation such that $c=a/\sqrt{2}$ would therefore indicate formation of the CsCl structure with a symmetric Pb site. This is in agreement with the experiment where PbO adopts the distorted litharge structure and PbS adopts the symmetric rocksalt structure, showing no stereochemical activity of the lone pair. To allow proper analysis of litharge, PbS additional optimizations were performed as a function of volume with constant a:c ratio taken from PbO with the resulting structure indicated in Table 1 (fixed a:c ratio).

The a and b lattice vector for litharge PbO and the lattice vector for rocksalt PbS are in good agreement with the experiment. The litharge c vector, which represents interlayer interactions in litharge, is overestimated to a greater extent due to the inability of DFT to accurately describe the non-bonding forces in this direction. However, the Pb–O interatomic distances are calculated to be 2.35 Å, within 1.5% of the experiment, and the stable phase is correctly predicted, indicating a good representation of the strong bonding and phase stability of PbO. The four Pb-anion nearest neighbour distances in the constrained litharge PbS are calculated at 2.82 Å. The rocksalt structure results in six Pb-anion distances of 2.63 Å in PbO and 3.01 Å in PbS within 1.3% of the experimentally determined value.

The electron densities were analysed for the states between −10 eV and the Fermi level. This removes the Pb 5d and O 2s (S 3s) states as they obscure the asymmetric density but do not contribute to it, or the bonding. Electron densities were plotted in the (100) plane passing through one lead atom in the centre for the rocksalt structure. Analysis of the electron density maps reveals that both PbO and PbS show symmetric

Table 1
Calculated data for rocksalt and litharge PbO and PbS and error with respect to experimental data where available

	PbO		PbS		
	Rocksalt	Litharge[a]	Rocksalt[b]	Litharge[c]	Litharge (fixed a:c)
Energy (eV/Pb)	−10.53	−10.91	−8.91	−8.61	−8.52
a (Å)	5.27	4.06 (+2.4%)	6.01 (+1.3%)	5.13	5.08
b (Å)	—	4.06 (+2.4%)	—	5.13	5.08
c (Å)	—	5.39 (+7.8%)	—	4.21	6.74
Pb–O (Å)	2.63	2.35 (+1.3%)	3.01 (+1.3%)	2.86	2.82

[a,b]% error with respect to experimental data, Ref. [2] and [4], respectively.
[c]This structure results from relaxation of PbS started from the litharge PbO structure scaled for the anion and relaxing toward the CsCl structure.

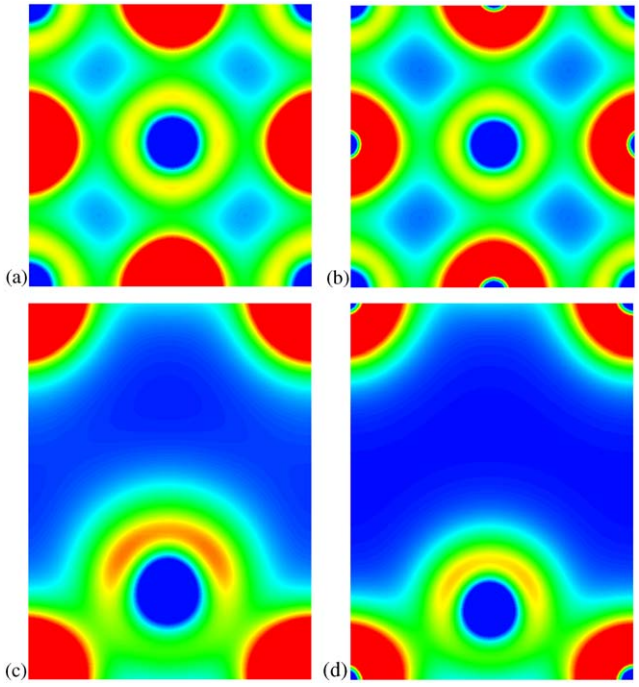

Fig. 2. Partial electron densities from −10 eV to the Fermi level for (a) rocksalt PbO, (b) rocksalt PbS, (c) litharge PbO and (b) litharge PbS plotted in the (100) plane and passing through four oxygen atoms (at the corners for litharge) and one Pb atom. Contour levels shown are between 0 (dark blue) and 0.375 e/Å^3 (red).

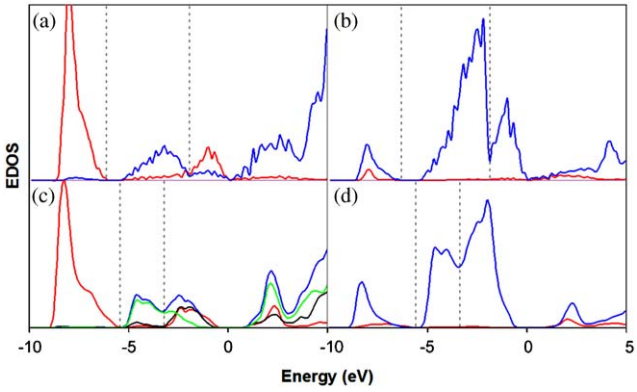

Fig. 3. Electronic density of states for (a) Pb and (b) O in rocksalt PbO and (c) Pb and (d) O in litharge PbO. The red lines correspond to s states, blue to p states, green to (p_x+p_y) and black p_z. The three regions of the valence band are represented by dashed lines.

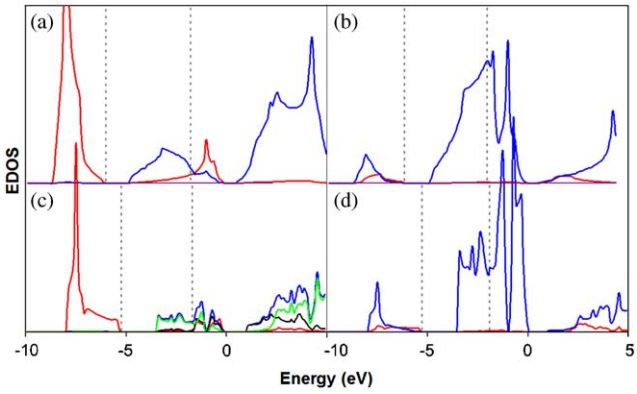

Fig. 4. Electronic density of states for (a) Pb and (b) S in rocksalt PbS and (c) Pb and (d) S in litharge PbS. The red lines correspond to s states, blue to p states, green to (p_x+p_y) and black p_z. The three regions of the valence band are represented by dashed lines.

electron densities in the rocksalt structure as expected (Fig. 2a and b). Electron densities were plotted in the (100) plane passing through four oxygen atoms (at the corners) and one lead atom for the litharge structure. Litharge PbO shows a marked asymmetric electron density directed into the space between the layers (Fig. 1a and 2c) while constrained litharge PbS displays similar but weaker asymmetry (Fig. 2d).

To examine the electronic structure in more detail we have calculated the partial (ion and l- and m-quantum number decomposed) electronic density of states (PEDOS). These were obtained by projecting the wave functions onto spherical harmonics centred on each atom with a radius of 1.55 Å for both Pb and O atoms and 1.85 Å for S atoms. These radii were chosen because they give rise to reasonable space filling, but the results (at least the qualitative aspects) are insensitive to a change of the radii.

Fig. 3 shows the PEDOS curves between −10 and +5 eV (relative to the Fermi level) for Pb and O in both rocksalt and litharge structures, while Fig. 4 shows the PEDOS for PbS. The basic structure of the EDOS are very similar with three main regions. The first region at around −8 eV is mainly Pb 6s but also contains some O 2p (or S 3p). The second is mainly O 2p (S 3p) with a small amount of Pb 6p. The region at the top of the valence band contains mainly O 2p (S 3p) but with some Pb 6s character. The underlying interactions can be investigated in more detail using integrated crystal orbital overlap populations [26] (COOP) for each material, which can be used to represent the bonding between two orbital centres. Positive and negative values correspond to bonding and antibonding interactions respectively. The integrated COOP values for the Pb 6s–anion p peaks, located around −8 eV (region I) and −1 eV (region III) are shown in Table 2. For rocksalt PbO region I corresponds to a filled bonding interaction (large, positive COOP) while region III corresponds to a filled antibonding combination (large, negative COOP) resulting from the Pb 6s and the O p states. In this way Pb 6s states are found at a substantially higher energy than expected, close to the Fermi level.

For litharge PbO there is an additional interaction. The high energy Pb 6s states formed through the filling of the antibonding Pb 6s–O 2p combination further

Table 2
Integrated COOP for the region I and region III Pb 6*s*–O 2*p* interaction and the region III Pb 6p_z–O 2*p* interaction

Interaction	Region	PbO		PbS	
		Rocksalt	Litharge	Rocksalt	Litharge
Pb 6*s*–O 2*p*	1	0.42	0.46	0.26	0.22
Pb 6*s*–O 2*p*	3	−0.40	−0.44	−0.28	−0.24
Pb 6p_z–O 2*p*	3	0.04	0.28	0.04	0.18

hybridize with Pb 6p_z. This can be seen in the PEDOS (Fig. 3c) in which Pb 6p_z overlaps with the Pb 6*s* and O 2*p* states in region III. Further evidence for this interaction is found in the unoccupied states in which, for litharge PbO, a Pb 6*s* peak is observed at +2 eV. For rocksalt, region III contains the highest energy 6s states, and as these correspond to filled antibonding levels there are no unfilled 6*s* states. Within the asymmetric environment of litharge, additional interaction with Pb 6*p* results in filled in phase and unfilled out of phase interactions. It is these unfilled out of phase interactions which results in the appearance of the 6*s* states above the Fermi level. The integrated COOP values confirm that while in rocksalt PbO no significant Pb 6p_z–O 2*p* interaction occurs, in litharge PbO a strong bonding interaction between Pb 6p_z and O 2*p* states takes place in region III. The interaction of Pb 6p_z with the antibonding combination close to the Fermi level results in a stabilization of these states and hence the structure, resulting in a shift of these peaks away from the Fermi level.

For rocksalt PbS, the bonding Pb 6*s*–S 3*p* states in region I of the PEDOS are significantly weaker than PbO with the integrated COOP, showing that the interaction has reduced to around 50% of that observed for O 2*p*. This leads to reduced antibonding states and thus there are significantly fewer Pb 6*s* states near the Fermi level. For litharge PbS the same reduction in the bonding and antibonding combinations can be seen (Table 2). With less antibonding states present at −1 eV the subsequent interaction of Pb 6p_z which occurs very strongly in litharge PbO is greatly diminished in litharge PbS, with the integrated COOP for the interaction reducing from 0.28 to 0.18.

The observed differences in the interactions can be supported by using partial electron density maps to visualize specific regions of the EDOS. The density maps for regions I and III are shown for litharge PbO and PbS in Fig. 5. A bonding interaction between Pb and O is visible for the low energy states with high electron density located between the atoms, Fig. 5a. The states in the highest occupied region are clearly responsible for the asymmetry observed in the Pb(II) electron density, Fig. 5b. A highly asymmetric lobe is directed away from

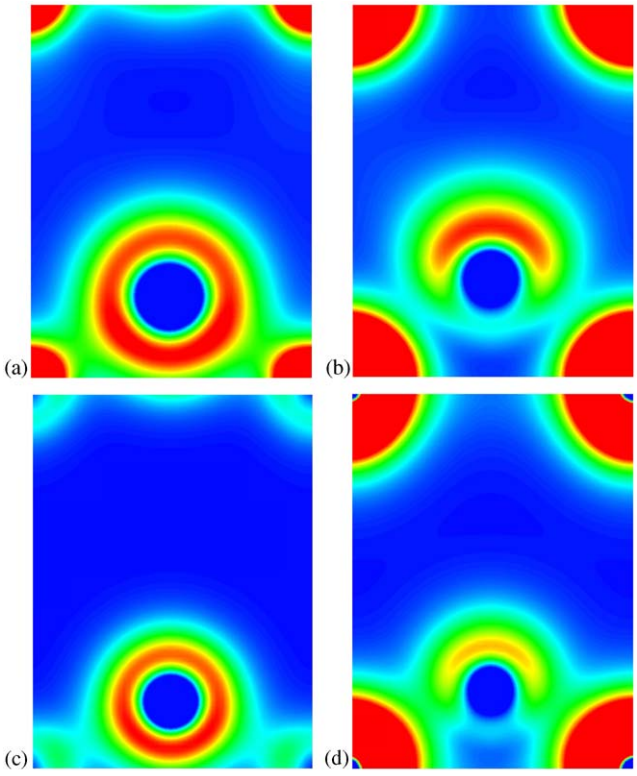

Fig. 5. Partial electron densities for the states between −9 and −6 eV (region I) and from −2.5 eV to the Fermi level (region III) for (a) region I and (b) region III for litharge PbO and (c) region I and (d) region III for PbS plotted in the (100) plane and passing through four oxygen atoms (at the corners) and one Pb atom. Contour levels shown are between 0 and 0.15 e/Å^3.

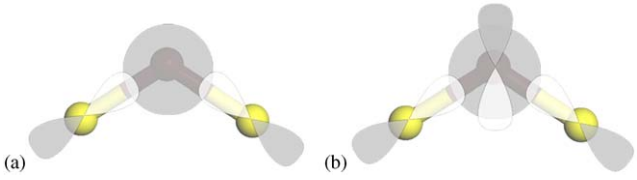

Fig. 6. Schematic orbital diagram for the litharge structure of (a) the out of phase Pb 6*s*–anion *p* interaction and (b) the subsequent interaction of Pb 6*p* with the out of phase combination.

Pb with the lack of density between O and Pb indicative of the antibonding nature of their interaction in this region. The symmetric electron distribution of rocksalt PbO indicates that the antibonding Pb 6*s* and O 2*p* states alone do not result in asymmetry in the Pb electron density, the subsequent interaction of Pb 6*p*, present in litharge PbO, is also required. The antibonding states originate from the filled out of phase combination from the interaction of Pb 6*s* and the anion *p*, shown schematically in Fig. 6a. The coupling of Pb 6p_z with these states enhances the Pb electron density through constructive interference of Pb 6*s* and Pb 6p_z on one side of the atom, away from the oxygen atoms,

resulting in the observed "lone pair", Fig. 6(b). On the opposite side the Pb electron density is thereby reduced through destructive interference, effectively reducing the antibonding interaction with O 2*p*.

For PbS, the low energy region has significantly less electron density on the anion, and between Pb and S, compared to PbO, Fig. 5c. The Pb density in this region remains almost spherical, indicating the dominance of the Pb 6*s* states and the reduced bonding in line with COOP analysis. The reduced states at the top of the valence band leads to weaker lone pair activity. There is significantly less density on the Pb atom in the high-energy region, responsible for the strong asymmetry in PbO, Fig. 5d. This corresponds to a reduction of antibonding states and the observed reduction in coupling with Pb 6*p* as observed in the PEDOS and COOP. The antibonding density is directed away from the sulphur layers in litharge PbS, but the asymmetry is much weaker than PbO. This can be understood with the transition of anion *p* states from O 2*p* to S 3*p*. The filled Pb 6*s* states are more stable than the anion *p* states and as such are positioned lower in energy. For oxygen, the 2*p* states are sufficiently low in energy to facilitate an interaction with Pb 6*s*, resulting in the strong bonding and antibonding combinations observed for PbO. However, for sulphur the transition to 3*p* increases the energy difference between Pb 6*s* and the anion *p* states hence decreasing their interaction. The stabilization resulting from the lone pair formation must off set the loss in energy due to a reduction in coordination number for litharge (four) compared with rocksalt (six). In the case of PbS the weak lone pair does not provide sufficient stabilization and hence rocksalt is the thermodynamically stable phase.

This analysis shows that coupling of Pb 6*p* with the antibonding Pb 6*s*–anion *p* states gives rise to the net asymmetry in the electron density on Pb. As the Pb 6*s* and 6*p* states are too distant in energy to couple directly, this coupling can only take place when there is an appropriate anion that can interact with Pb 6*s* generating Pb 6*s* states close to the Fermi level. Oxygen has the required energy levels to achieve this while sulphur does not. The directed asymmetric density produced by PbS is therefore weak and cannot stabilize the distorted structure relative to a symmetric structure of higher coordination, explaining why rocksalt is the thermodynamically stable phase of PbS. The formation of the asymmetric electron density in Pb(II) therefore depends on both the cation and anion, showing that the sterically active lone pair is chemically dependent.

4. Conclusions

In this study we have calculated for the first time the detailed electronic structure of both PbO and PbS in the rocksalt and litharge structures using DFT, and correctly identified their stable crystal structures. We have demonstrated using partial electron densities of states, COOP analysis and partial electron densities that the asymmetric electron density formed by Pb(II), in contrast to traditional lone pair theory, is a result of the interaction of the antibonding combination of Pb 6*s* and anion *p* states with unfilled Pb 6*p*. In the case of litharge PbO this causes a shift of the states at the Fermi level to lower energy and the appearance of unoccupied Pb 6*s* states in the conduction band. Similar but weaker antibonding states are observed for constrained litharge PbS indicating that strong Pb 6*p* coupling does not occur. This is shown to be a result of weaker interaction between Pb 6*s* and S 3*p* due to the higher energy of S 3*p* compared to O 2*p* with the lack of antibonding Pb 6*s* states reducing the coupling with Pb 6*p*. The weak asymmetry produced for litharge PbS cannot stabilize the distorted structure over six coordinate rocksalt which explains why PbS does not adopt the litharge structure experimentally. These results show that the so-called Pb(II) inert lone pair is a direct result of cation–anion interactions, having major implications for understanding and tuning the properties of materials that display such asymmetric electron densities.

Acknowledgments

We would like to acknowledge the HEA for a PRTLI (Cycle III) grant and Trinity College for a TCD postgraduate studentship. We would also like to thank Dr. Peter Oliver at Rutherford Appleton Laboratory for access and assistance with Hrothgar, a 16 node Beowulf cluster.

References

[1] L.E. Orgel, J. Chem. Soc. 1959 (1959) 3815.
[2] J. Leciejewicz, Acta Cryst. 14 (1961) 1304.
[3] J. Hill, Acta Cryst. 41 (1985) 1281.
[4] Y. Noda, S. Ohba, S. Sato, Y. Saito, Acta. Cryst. B 39 (1983) 312.
[5] M. Veith, J. Hans, L. Stahl, P. May, V. Huch, Z. Sebald, Z. Natureforsch. B 46 (1991) 403.
[6] F. Cecconi, C.A. Ghilardi, S. Midollini, A. Orlandini, Inorg. Chem. Acta 398 (2000) 135.
[7] H.U. Hummel, H. Meske, Z. Natureforsch. B 44 (1989) 293.
[8] L.M. Engelhardt, B.M. Furphy, J.McB. Harrowfield, J.M. Patrick, B.W. Skelton, A.H. White, J. Chem. Soc. Dalton Trans. 1989 (1989) 565.
[9] D.L. Reger, C.A. Little, M.D. Smith, A.L. Rheingold, L.M. Liable-Sands, G.P.A. Yap, I.A. Guzei, Inorg. Chem. 41 (2002) 19.
[10] L. Shimoni-Livny, J.P. Glusker, C.B. Bock, Inorg. Chem. 37 (1998) 1853.
[11] L. Bernasconi, M. Wilson, P.A. Madden, Comp. Mat. Sci. 22 (2001).
[12] G. Trinquier, R. Hoffmann, J. Phys. Chem. 88 (1984) 6696.
[13] H.J. Terpstra, R.A. de Groot, C. Haas, Phys. Rev. B 52 (1995) 11690.

[14] G.W. Watson, S.C. Parker, J. Phys. Chem. B 103 (1999) 1258.
[15] G.W. Watson, S.C. Parker, G. Kresse, Phys. Rev. B 59 (1999) 8481.
[16] G.W. Watson, J. Chem. Phys. 114 (2001) 758.
[17] A. Walsh, G.W. Watson, Phys. Rev. B 70 (2004) 235114.
[18] U. Haussermann, P. Berastegui, S. Carlson, J. Haines, J.M. Leger, Angew. Chem. Int. Edit. 40 (2001) 4624.
[19] J.M. Raulot, G. Baldinozzi, R. Seshadri, P. Cortona, Sol. State Sci. 4 (2002) 467–474.
[20] U.V. Waghmare, N.A. Spaldin, H.C. Kandpal, R. Seshadri, Phys. Rev. B 67 (2003) 125111.
[21] G. Kresse, J. Furthmüller, Phys. Rev. B 54 (1996) 11169.
[22] G. Kresse, J. Furthmüller, Comput. Mater. Sci. 6 (1996) 15.
[23] J.P. Perdew, K. Burke, M. Ernzerhof, Phys. Rev. Lett. 77 (1996) 3865.
[24] G. Kresse, J. Joubert, Phys. Rev. B 59 (1999) 1758.
[25] G. Kresse, VASP Manual, Section 9.6, http://www.cms.mpi.univie.ac.at/vasp/guide/node161.html
[26] R. Hoffmann, Solids and Surfaces, Wiley-VCH, New York, 1988, p. 42.